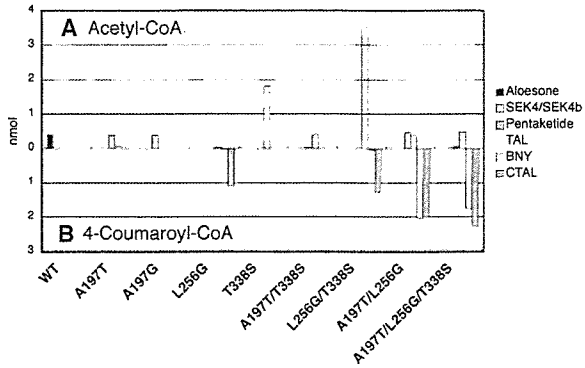

Fig. 7. Polyketide product distribution pattern of ALS and its mutants: (A) acetyl-CoA and (B) 4-coumaroyl-CoA as a starter substrate in the assay mixture. Quantification of the products was calculated from the ^{14}C incorporation rate from [2-^{14}C]malonyl-CoA under the standard assay condition.

superfamily enzyme. The type III PKSs are structurally and mechanistically distinct from the modular type I and the iterative type II PKSs of bacterial origin; the simple homodimer of 40–45 kDa proteins catalyse complete series of polyketide formation reactions from the CoA-linked substrates with a single active site of the Cys-His-Asn catalytic triad [1,2].

The simple steric modulation of the active site cavity by the three residues, Ala197, Leu256, and Thr338, is crucial for the remarkable catalytic activity of *R. palmatum* ALS. The site-directed mutagenesis revealed that even a single amino acid replacement at these positions (A197T, L256G, and T338S) completely abolished the heptaketide-forming activity. Further, a combination of the three amino acid substitutions (A197T/L256G/T338S) modulates between formation of the heptaketide aloesone from acetyl-CoA starter and a tetraketide CTAL from 4-coumaroyl-CoA.

It was demonstrated that the 'horizontally restricting' (2PS-like) G256L substitution [9,20] controls the starter substrate selectivity in *R. palmatum* ALS (Fig. 3). The small-to-large replacement interrupts the loading of the bulky 4-coumaroyl-CoA at the active site, but allows access of the smaller acetyl-CoA starter. Indeed, when Leu256 of ALS was substituted with less bulky Gly, L256G mutant now accepted 4-coumaroyl-CoA as a starter to efficiently produce CTAL, whereas wild-type ALS did not accept the coumaroyl starter.

On the other hand, the 'downward expanding' T197A replacement [21] facilitates the enzyme to carry out the six successive condensations with malonyl-CoA (Fig. 3). Interestingly, the heptaketide-producing ALS was converted to a pentaketide synthase by A197T substitution, whereas A197G mutant yielded octaketides SEK4/SEK4b [18,19]. Remarkably, the single amino acid residue 197 determines the polyketide chain length, as in the case of *A. arborescens* PCS [18] and *A. arborescens* OKS [19]. The homology model predicted that the gate to the buried pocket that extends into the active site floor is more widely open in the octaketide-producing A197G than in the pentaketide-producing A197T mutant (Fig. 4C, D). Very recently, we have solved crystal structures of *A. arborescens* PCS, both the pentaketide-producing wild-type and the octaketide-producing M197G mutant enzyme (H. Morita, S. Kondo, S. Oguro, H. Noguchi, S. Sugio, T. Kohno, I. Abe, unpublished data). The crystal structures at 1.6-Å resolution revealed that the residue 197 lining the active site cavity is indeed located at the entrance of an additional buried pocket.

Mechanistically, as in the case of the previously reported *A. arborescens* OKS [19], both wild-type and the mutant ALS are likely to catalyse chain elongation and the first aromatic ring formation reaction at the methyl end of the polyketide intermediate (Fig. 5A–C). The partially cyclized intermediates would be then released from the active site, and undergo subsequent spontaneous cyclizations, thereby completing the formation of the fused ring systems.

Finally, Thr338 located in proximity of the catalytic Cys164 at the 'ceiling' of the active site cavity (Fig. 4) also plays a crucial role in the polyketide chain elongation reactions in *R. palmatum* ALS. It is surprising that a single amino acid substitution T338S, just a removal of a methyl group from the side chain of Thr, completely abolished the aloesone-forming activity, and just afforded triketide TAL. Presumably, Thr338 provides steric guidance so that the linear polyketide intermediate tethered at the catalytic Cys164 extends into the buried pocket, thereby leading to formation of the longer polyketides (Fig. 3C, D). Very surprisingly, it was recently demonstrated that *Scutellaria baicalensis* CHS S338V point mutant produced a trace amount of SEK4/SEK4b in addition to 5,7-dihydroxy-2-methylchromone (I. Abe, T. Watanabe, H. Morita, T. Kohno, H. Noguchi, unpublished data). On the other hand, as ALS T338S mutant did not totally accept 4-coumaroyl-CoA as in the case of wild-type enzyme, the residue 338 is apparently not very important for the starter substrate selectivity.

In summary, we have identified the active site residues that control starter substrate selectivity and polyketide chain length in the heptaketide-producing *R. palmatum* ALS. Further, a CHS-like triple mutation (A197T/L256G/T338S) functionally converted ALS into a tetraketide CTAL-producing enzyme from 4-coumaroyl-CoA starter. These results provided

structural basis for understanding the functional diversity of type III PKS enzymes, and suggest strategies for engineered biosynthesis of plant polyketides.

Experimental procedures

Chemicals

[2-^{14}C]Malonyl-CoA (48 mCi·mmol^{-1}) and [1-^{14}C]acetyl CoA (47 mCi·mmol^{-1}) was purchased from Moravek Biochemicals (Brea, CA, USA). Malonyl-CoA and acetyl-CoA were purchased from Sigma. 4-Coumaroyl-CoA was chemically synthesized as described previously [24]. Authentic samples of 2,7-dihydroxy-5-methylchromone [19] and SEK4/SEK4b [18] were obtained in our previous works.

Site-directed mutagenesis

Rheum palmatum ALS mutants (A197T, A197G, L256G, T338S, A197T/L256G, L256G/T338S, A197T/T338S, A197T/L256G/T338S) (numbering in *M. sativa* CHS) were constructed using the QuickChange Site-Directed Mutagenesis Kit (Stratagene, La Jolla, CA, USA) and a pair of complementary mutagenic primers as follows (mutated codons are underlined): A197T, sense 5′-ATCGTGGCCTTCACCT TCCGCGGGCCCCAC-3′, antisense 5′-GTGGGGCCCGC GGAAGGTGAAGGCCACGAT-3′; A197G sense 5′-ATC GTGGCCTTCGGCTTCCGCGGGCCCCAC-3′, antisense 5′-GTGGGGCCCGCGGAAGCCGAAGGCCACGAT-3′; L256G, sense 5′-CACACCATGGCTGGCCATCTGACGG AGGCG-3′, antisense 5′-CGCCTCCGTCAGATGGCCA GCCATGGTGTG-3′; T338S, sense 5′-TACGGGAATCT CTCCAGCGCCTGTGTGCTC-3′, antisense 5′-GAGCA CACAGGCGCTGGAGAGATTCCCGTA-3′. The ALS mutant cDNA constructs were in the *Nde* I/*Sal* I site of pET-22b(+) (Novagen, San Diego, CA, USA) [15]. Thus, the recombinant enzymes contain an additional hexahistidine tag at the C terminus.

Enzyme expression and purification

After confirmation of the sequence, the plasmid was transformed into *Escherichia coli* BL21(DE3)pLysS. The cells harbouring the plasmid were cultured to an A_{600} of 0.6 in Luria–Bertani medium containing 100 μg·mL^{-1} of ampicillin at 30 °C. Then, 0.4 mM isopropyl thio-β-D-galactoside was added to induce protein expression, and the culture was incubated further at 16 °C for 14 h. The *E. coli* cells were harvested by centrifugation and resuspended in 40 mM potassium phosphate buffer pH 7.9, containing 0.1 M NaCl. Cell lysis was carried out by sonication, and centrifuged at 15 000 *g* for 40 min. The supernatant was passed through a column of Pro-Bond™ resin (Invitrogen, Carlsbad, CA, USA) containing Ni^{2+} as an affinity ligand. After washing with 20 mM potassium phosphate buffer, pH 7.9, containing 0.5 M NaCl and 40 mM imidazole, the recombinant ALS was finally eluted with 15 mM potassium phosphate buffer, pH 7.5, containing 10% glycerol and 500 mM imidazole. Protein concentration was determined by the Bradford method (Protein Assay, Bio-Rad, Hercules, CA, USA) with BSA as standard.

Enzyme reaction

The standard reaction mixture contained 27 nmol of starter CoA (acetyl-CoA or 4-coumaroyl-CoA) and 54 nmol of malonyl-CoA, and 460 pmol of the purified recombinant enzyme in a final volume of 500 μL of 100 mM potassium phosphate buffer pH 7.0. Incubations were carried out at 30 °C for 12 h, and stopped by adding 50 μL of 20% HCl. The products were then extracted with 1000 μL of ethyl acetate, and concentrated by N_2 flow. The residue was dissolved in aliquot of MeOH containing 0.1% trifluoroacetic acid (TFA), and separated by reverse-phase HPLC (JASCO 880, Tokyo, Japan) on a TSK-gel ODS-80Ts column (4.6 × 150 mm, TOSOH) with a flow rate of 0.8 mL·min^{-1}. Gradient elution was performed with H_2O and MeOH, both containing 0.1% TFA: 0–5 min, 30% MeOH; 5–17 min, linear gradient from 30 to 60% MeOH; 17–25 min, 60% MeOH; 25–27 min, linear gradient from 60 to 70% MeOH. Elutions were monitored by a multichannel UV detector (MULTI 340, JASCO) at 290 nm, 330 nm and 360 nm; UV spectra (198–400 nm) were recorded every 0.4 s.

On-line LC-ESIMS spectra were measured with a Hewlett-Packard HPLC 1100 series (Wilmington, DE, USA) coupled to a Finnigan MAT LCQ ion trap mass spectrometer (San Jose, CA, USA) fitted with an ESI source. HPLC separations were carried out under the same conditions as described above. The ESI capillary temperature and capillary voltage were 225 °C and 3.0 V, respectively. The tube lens offset was set at 20.0 V. All spectra were obtained in both negative and positive mode over a mass range of *m/z* 100–500. The collision gas was helium, and the relative collision energy scale was set at 30.0% (1.5 eV).

Enzyme kinetics

Steady-state kinetic parameters were determined by using [2-^{14}C]malonyl-CoA (1.8 mCi·mmol^{-1}) as a substrate. The experiments were carried out in triplicate using four concentrations (10.8, 21.6, 32.4, 43.2, and 54 μM) of the starter substrate (acetyl-CoA or 4-coumaroyl-CoA) in the assay mixture, containing 108 μM of malonyl-CoA, 4.4 μg of purified enzyme, 1 mM EDTA, in a final volume of 500 μL of 100 mM potassium phosphate buffer. Incubations were carried out at 30 °C for 30 min. The reaction products were extracted and separated by Si-gel TLC (Merck Art. 1.11798; ethyl acetate/hexane/AcOH = 63 : 27 : 5, v/v/v).

Radioactivities were quantified by autoradiography using a bioimaging analyzer BAS-2000II (FUJIFILM, Tokyo, Japan). The enzyme activities were calculated for the starter substrates. Lineweaver-Burk plots of data were employed to derive the apparent K_M and k_{cat} values (average of triplicates$^+$-standard deviation) using EnzFitter software (BIOSOFT, Cambridge, UK).

Homology modelling

The model was produced by the SWISS-MODEL package (http://expasy.ch/spdbv/) provided by the Swiss-PDB-Viewer program [25]. A standard homology modelling procedure was applied based on the sequence homology of *R. palmatum* ALS and the X-ray crystal structures of *M. sativa* CHS including wild-type (1BI5A.pdb, 1BQ6A.pdb, 1CGKA.pdb, 1CGZA.pdb, 1CHWA.pdb, 1CHWB.pdb, 1CMLA.pdb), C164A mutant (1D6FA.pdb), N336A mutant (1D6HA.pdb), H303Q mutant (1D6IA.pdb, 1D6IB.pdb), G256A mutant (1I86A.pdb), G256V mutant (1I88A.pdb, 1I88B.pdb), G256L mutant (1I89A.pdb, 1I89B.pdb), G256F mutant (1I8BA.pdb, 1I8BB.pdb), and F215S mutant (1JWX.pdb). The corresponding Ramachandran plot was also created with Swiss PDB-Viewer software to confirm that the majority of residues grouped in the energetically allowed regions. Calculation of the total cavity volumes (Connolly's surface volumes) was then performed with CASTP program (http://cast.engr.uic.edu/cast/) [26].

Acknowledgements

This work was in part supported by the COE21 Program, Grant-in-Aid for Scientific Research (Nos. 16510164, 17310130, and 17035069), and Cooperation of Innovative Technology and Advanced Research in Evolutional Area (CITY AREA)-in the Central Shizuoka Area-, from the Ministry of Education, Culture, Sports, Science and Technology, Japan, and by Health and Labour Sciences Research Grant from the Ministry of Health, Labour and Welfare, Japan.

References

1 Schröder J (1999) The chalcone/stilbene synthase-type family of condensing enzymes. *Comprehensive Natural Products Chemistry*, **Vol. 1**, pp. 749–771. Elsevier, Oxford.
2 Austin MB & Noel JP (2003) The chalcone synthase superfamily of type III polyketide synthases. *Nat Prod Report* **20**, 79–110.
3 Austin MB, Bowman ME, Ferrer J-L, Schröder J & Noel JP (2004) An aldol switch discovered in stilbene synthases mediates cyclization specificity of Type III polyketide synthases. *Chem Biol* **11**, 1179–1194.
4 Kreuzaler F & Hahlbrock K (1975) Enzymatic synthesis of aromatic compounds in higher plants. Formation of bis-noryangonin (4-hydroxy-6-[4-hydroxystyryl]2-pyrone) from *p*-coumaroyl-CoA and malonyl-CoA. *Arch Biochem Biophys* **169**, 84–90.
5 Akiyama T, Shibuya M, Liu HM & Ebizuka Y (1999) *p*-Coumaroyltriacetic acid synthase, a new homologue of chalcone synthase, from *Hydrangea macrophylla* var. *thunbergii*. *Eur J Biochem* **263**, 834–839.
6 Ferrer JL, Jez JM, Bowman ME, Dixon RA & Noel JP (1999) Structure of chalcone synthase and the molecular basis of plant polyketide biosynthesis. *Nat Struct Bio* **6**, 775–784.
7 Jez JM, Ferrer JL, Bowman ME, Dixon RA & Noel JP (2000) Dissection of malonyl-coenzyme A decarboxylation from polyketide formation in the reaction mechanism of a plant polyketide synthase. *Biochemistry* **39**, 890–902.
8 Jez JM & Noel JP (2000) Mechanism of chalcone synthase: pKa of the catalytic cysteine and the role of the conserved histidine in a plant polyketide synthase. *J Biol Chem* **275**, 39640–39646.
9 Jez JM, Bowman ME & Noel JP (2001) Structure-guided programming of polyketide chain-length determination in chalcone synthase. *Biochemistry* **40**, 14829–14838.
10 Tropf S, Kärcher B, Schröder G & Schröder J (1995) Reaction mechanisms of homodimeric plant polyketide synthase (stilbenes and chalcone synthase). A single active site for the condensing reaction is sufficient for synthesis of stilbenes, chalcones, and 6′- deoxychalcones. *J Biol Chem* **270**, 7922–7928.
11 Suh DY, Fukuma K, Kagami J, Yamazaki Y, Shibuya M, Ebizuka Y & Sankawa U (2000) Identification of amino acid residues important in the cyclization reactions of chalcone and stilbene synthases. *Biochem J* **350**, 229–235.
12 Suh DY, Kagami J, Fukuma K & Sankawa U (2000) Evidence for catalytic cysteine-histidine dyad in chalcone synthase. *Biochem Biophys Res Commun* **275**, 725–730.
13 Jez JM, Bowman ME & Noel JP (2002) Expanding the biosynthetic repertoire of plant type III polyketide synthases by altering starter molecule specificity. *Proc Natl Acad Sci USA* **99**, 5319–5324.
14 Abe I, Sano Y, Takahashi Y & Noguchi H (2003) Site-directed mutagenesis of benzalacetone synthase. The role of the Phe215 in plant type III polyketide synthases. *J Biol Chem* **278**, 25218–25226.
15 Abe I, Utsumi Y, Oguro S & Noguchi H (2004) The first plant type III polyketide synthase catalyzing formation of aromatic heptaketide. *FEBS Lett* **562**, 171–176.
16 Abe I, Takahashi Y, Morita H & Noguchi H (2001) Benzalacetone synthase. A novel polyketide synthase that plays a crucial role in the biosynthesis of phenyl-

butanones in *Rheum palmatum*. *Eur J Biochem* **268**, 3354–3359.
17 Eckermann S, Schröder G, Schmidt J, Strack D, Edrada RA, Helariutta Y, Elomaa P, Kotilainen M, Kilpeläinen I, Proksch P, Teeri TH & Schröder J (1998) New pathway to polyketides in plants. *Nature* **369**, 387–390.
18 Abe I, Utsumi Y, Oguro S, Morita H, Sano Y & Noguchi H (2005) A plant Type III polyketide synthase that produces pentaketide chromone. *J Am Chem Soc* **127**, 1362–1363.
19 Abe I, Oguro S, Utsumi Y, Sano Y & Noguchi H (2005) Engineered biosynthesis of plant polyketides: chain length control in an octaketide-producing plant Type III polyketide synthase. *J Am Chem Soc* **127**, 12709–12716.
20 Jez JM, Austin MB, Ferrer J, Bowman ME, Schröder J & Noel JP (2000) Structural control of polyketide formation in plant-specific polyketide synthases. *Chem Biol* **7**, 919–930.
21 Funa N, Ohnishi Y, Fujii I, Shibuya M, Ebizuka Y & Horinouchi S (1999) A new pathway for polyketide synthesis in microorganisms. *Nature* **400**, 897–899.
22 Austin MB, Izumikawa M, Bowman ME, Udwary DW, Ferrer J-L, Moore BS & Noel JP (2004) Crystal structure of a bacterial Type III polyketide synthase and enzymatic control of reactive polyketide intermediates. *J Biol Chem* **279**, 45162–45174.
23 Sankaranarayanan R, Saxena P, Marathe U, Gokhale RS, Shanmugam VM & Rukmini R (2004) A novel tunnel in mycobacterial type III polyketide synthase reveals the structural basis for generating diverse metabolites. *Nat Struct Mol Biol* **11**, 894–900.
24 Abe I, Morita H, Nomura A & Noguchi H (2000) Substrate specificity of chalcone synthase: enzymatic formation of unnatural polyketides from synthetic cinnamoyl-CoA analogues. *J Am Chem Soc* **122**, 11242–11243.
25 Guex N & Peitsch MC (1997) SWISS-MODEL and the Swiss-PdbViewer: An environment for comparative protein modeling. *Electrophoresis* **18**, 2714–2723.
26 Liang J, Edelsbrunner H & Woodward C (1998) Anatomy of protein pockets and cavities: measurement of binding site geometry and implications for ligand design. *Protein Sci* **7**, 1884–1897.